International Journal of Integrated Engineering, Vol. 3 No. 1 (2011) p. 17-22

Analysis of Sensitization Profile in Medium Chromium Ferritic Stainless Steel (FSS) Welds

M.O.H. Amuda[1,*] and S. Mridha[1]

[1]Advanced Materials and Surface Engineering Research Unit (AMSERU), Department of Manufacturing and Materials Engineering, International Islamic University Malaysia, P.O. Box 10, 50728, Kuala Lumpur, Malaysia.

Received 15 June 2011; accepted 2 August 2011, available online 21 September 2011

Abstract: The sensitization features in Ferritic Stainless Steel (FSS) welds are discussed in the present work. The welds were produced on a 1.5mm thick plate of 16wt%Cr FSS conforming to AISI 430 commercial grade, using TIG torch in argon environment at a heat flux between 1008W and 1584W and speed between 2.5mm/s and 3.5mm/s. The sensitization was evaluated by electrolytic etching of the weld cross sections in 10% oxalic acid. The characterization of the weld section for sensitization indicates that the size of the sensitized zone increases in direct proportion to the quantum of the heat input (combination of heat flux and welding speed). Microstructural analysis suggests that sensitization is promoted in the welds when the processing conditions (heat flux and welding speed) restricts the transformation occurring during cooling through the dual phase region, i.e. the welding conditions that promote transformation of delta ferrite (δ) to austenite (γ) during cooling cycle can prevent sensitization in the FSS welds and such conditions found in this investigation correspond to welding with a heat flux in the range 1008W to 1296W and speed 3mm/s to 3.5mm/s. These conditions of heat fluxes and welding speeds correspond to heat inputs in the range 288-432J/mm.

Keywords: Sensitization features, welding conditions, austenite, FSS weld, thermal cycle.

1. Introduction

The medium chromium FSS represents a group of iron-chromium steels containing nominal chromium content in the range 16-18wt% and nickel at less than 4wt% [1]. They exhibit slightly higher mechanical property relative to the low chromium group and readily find application in automotive exhaust systems, electronic system against electromagnetic radiation, regenerators, boiler linings, etc. More significantly is that, as typical of FSS, they exhibit better stress corrosion cracking resistance as well as superior resistance to pitting and crevice corrosion in chloride environment than the often used austenitic grades [2]. They equally have additional property advantages over the austenitics in such areas as improved machinability, higher thermal conductivity and lower thermal expansion [1]. These grades provide a saving of approximately 1.5 percent over the austenitic grades in material cost and are, as such, attractive alternative to the austenitic variety [3].

But this grade of stainless steel is not commonly used for structural engineering purposes because their fabrication is associated with several challenges principal among which is the deterioration in after-weld properties following conventional fusion welding process. However, in the recent past, the austenitic variety is becoming quite expensive on the account of the increasing cost of nickel; a major alloying element. Therefore, there is a renewed interest in the FSS though the challenges of acceptable weldability have yet to be fully addressed [4].

Different welding techniques have been explored to improve weldability of the ferritics and it emerged that low heat input processes provides a promise [5]. Yet the range of process variables that can be classified as low heat input is not universally established. In furtherance of this, the authors [6] recently investigated the effect of certain range of currents and welding speeds on microstructures and properties of 1.5mm thick medium chromium FSS welds. The work indicates that current range 70-110A and welding speeds 2.5-3.5mm/s provides the best combination of metallurgical features and mechanical properties.

Meanwhile, apart from the loss of ductility in FSS welds due to fusion welding, the steel is also susceptible to sensitization. This is the loss in corrosion strength due to the depletion of chromium content below the level necessary for resistance/passivity. It is necessary to know the sensitization behaviour of the steel under these optimized welding conditions in order to have a wholesome knowledge of the features and properties of the weld section under these conditions.

Therefore, in the current paper, the sensitization behaviour in medium chromium FSS welds under different heat fluxes and welding speeds within the domain of the optimized conditions is reported.

2. Experimental Method

A cold rolled medium chromium FSS conforming to AISI 430 specification was used for this investigation. The material received in the form of 1.5mm thick sheet was cut into coupons of dimensions 65 mm x 25 mm. The

*Corresponding author: mwalehakeem@gmail.com

chemical composition of the steel provided by the supplier and complemented with X-ray fluorescence is given in Table 1 together with the Kaltenhauser ferrite factor (KFF). The KFF is a rating factor that determines the tendency to form martensite in FSS welds; since martensite in welds microstructure is reported to assist in the control of sensitization by taking carbon into solution [7].

Table 1 Chemical composition of AISI 430 FSS (%by mass, balance Fe).

Material Spec.	Composition							
	C	Cr	Si	Mn	P	S	Ti	Fe
AISI 430	0.12	16.19	0.75	1.0	0.04	0.30	-	Balance

Autogenous full weld bead on coupon was produced using direct current straight polarity (DCEN) arc torch from a Miller-Telwin 165 TIG welding machine (see Fig.1). The effective heat input to produce weld track under different currents and traverse speed was calculated using the expression provided in Eqs. 1 and 2, respectively

$$q = \eta I V \qquad (1)$$

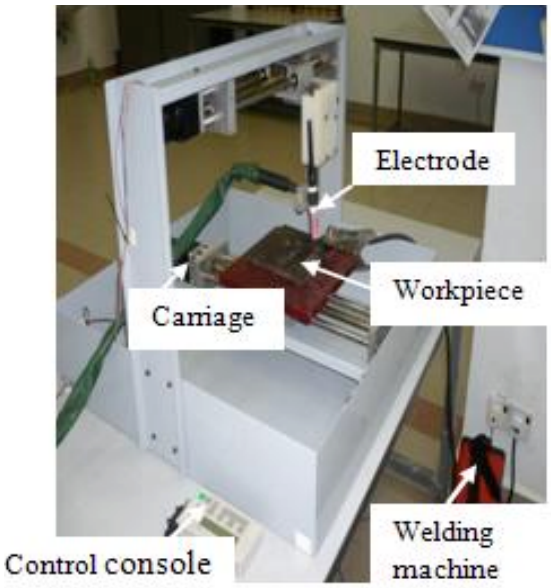

Fig. 1Welding rig.

$$HI = \frac{q}{v} \qquad (2)$$

where q is the heat flux (W), η is the process efficiency which for TIG welding is roughly 0.48 [8], I is the arc current (A), V is the voltage (V) and υ is the welding speed (mm/s). The voltage in the present investigation was relatively fixed at 30V.

A standard technique was used to prepare metallographic sample of the resolidified weld cross sections.

Table 2 Welding conditions for sensitization studies.

Run	Current (A)	Welding Speed (mm/s)	Arc Voltage (V)	Heat Input (J/mm)	Argon Gas Flow Rate (L/min)
1	90	3.5	30	370.29	0.72
2	70	3.5	30	288.00	0.72
3	110	3.0	30	528.00	0.72
4	90	3.0	30	432.00	0.72
5	90	2.5	30	518.40	0.72
6	110	3.5	30	452.60	0.72
7	70	2.5	30	403.20	0.72
8	70	3.0	30	336.00	0.72
9	110	2.5	30	633.60	0.72

The influences of welding parameters (arc current and welding speeds) on chromium carbide precipitation in the heat affected zone (HAZ) were studied by conducting test on selected weld pools produced under different conditions. The conditions of the heat input considered are provided in Table 2. The investigation was based on 3^k factorial experimental design which is suitable for planning experiment with k factors, each at three levels.

(a)

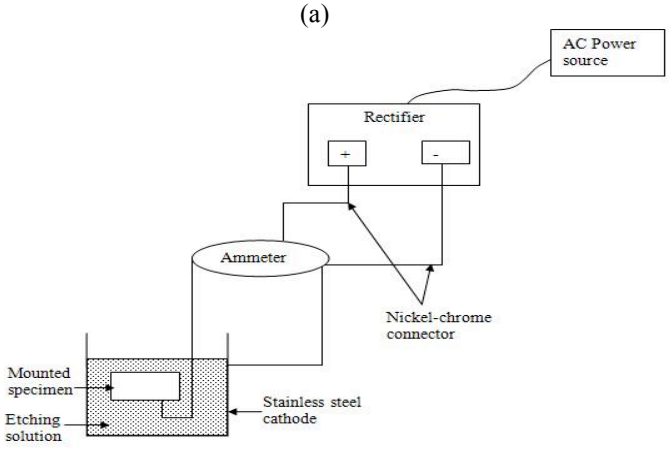

(b)

Fig. 2 Set-up for 10% oxalic acid etch: (a) the physical system build-up and (b) line diagram for the test.

Sensitization of the weld structure was investigated using ASTM A763-93 standard [9]. In this method, the polished cross section of the weld pool was etched electrolytically in 10% oxalic acid solution using 1 A/cm^2 for 1.5 minutes. The etched samples were then examined under Nikon Epiphot 200 optical microscope with image analysis software. The experimental set-up and the line diagram for the electrolytic etch test is shown in Fig. 2.

3. Results and Discussion

Sensitization occurs in regions of the HAZ exposed to peak temperatures in the range 650-950^{0}C for a short period during the welding process. The sensitized region is located at a fixed point from the weld interface; and the width and depth extend few millimeters both in the lateral and transverse section, respectively [10]. A physical illustration of the sensitization profile in the weld section is presented in Fig. 3. The broken line represents the boundary of the sensitized zone, x_1 is the width of the fusion zone, x_2 is the location of the sensitized zone from the weld interface and x_3 is the width of the sensitized zone in the lateral dimension. Similar notation in the transverse section is indicated in the figure.

The location of the sensitization zone from the weld interface and its geometry were evaluated using low magnification Nikon MM-400L trinocular head measuring microscope and the results in Table 3 show that the sensitization profile changes in direct proportion to the welding conditions. The width of the sensitization zone varies from zero to 1.6mm. The sensitization width in the weld track made with heat input below 400J/mm is less than 0.5mm. Indeed, weld tracks made with a heat input of 432J/mm show no sensitization zone. However, in tracks made with a heat input greater than 452J/mm, the width can be as high as 1.6mm. This is around 67% of the size of the HAZ. This shows that welding with higher heat input increases the size of the sensitized region within the HAZ. The sensitization depth in the thickness direction is insignificant; basically not more than 0.5mm.

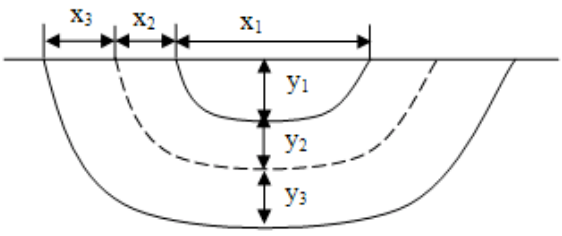

Fig. 3 Schematic representation of sensitization profile in weld section.

Other than the peak temperature, the time spent within the thermal cycle is critical in the development of the sensitized zone [10]. The track that exhibits a small sensitization width spend less than 9s in the sensitization temperature range as indicated in Table 3 whereas the heavily sensitized track spend more than 9s.

Table 3 Influence of welding conditions on sensitization profile.

Run	Current (A)	Heat Flux (W)	Welding Speed (mm/s)	Heat Input (J/mm)	Cooling time (s) $\Delta t_{1500-800}$	HAZ (mm)	x_2 (mm)	x_3 (mm)	y_2 (mm)	y_3 (mm)
1	90	1296	3.5	370	6.31	1.58	0.2	0.4	0	0.3
2	70	1008	3.5	288	3.82	1.52	0	0.2	0	0
3	110	1584	3.0	528	12.84	2.0	0.4	1.3	0.4	0.3
4	90	1296	3.0	432	8.59	1.84	0	0	0	0
5	90	1296	2.5	518	12.37	2.07	0.5	1.3	0	0.4
6	110	1584	3.5	452	9.43	1.61	0.3	0.9	0.1	0.4
7	70	1008	2.5	403	7.49	1.83	0.2	0.4	0.2	0.5
8	70	1008	3.0	336	5.20	1.72	0.2	0.3	0	0
9	110	1584	2.5	634	18.40	2.40	0.7	1.6	0.2	0.5

The heat fluxes are classified as low (1008W), intermediate (1296W) and high (1584W) in order to simplify the presentation and analyses of the response of the microstructure to oxalic acid etch. The heat input associated with each of the heat fluxes and the welding speeds is provided in Table 4. The table shows three bands of heat input: 288-370J/mm; 403-452J/mm; and 518-634J/mm, respectively.

Table 4 Stratification of the heat flux and welding speed.

Heat Flux (W)	Heat input (J/mm)		
	2.5mm/s	3mm/s	3.5mm/s
1008	403	336	288
1296	518	432	370
1584	634	528	452

ASTM 763-93, Practice W [9], provides acceptance criteria for oxalic acid etch depending on the state of the grain boundary. The detail of the classification is presented in Table 5 and these criteria are used to screen the microstructure of the HTHAZ of the weld section for susceptibility to sensitization.

Table 5 Classification of microstructure in 10% oxalic acid electrolytic etch [9].

Classification	State of the microstructure
Acceptable	i. *Step structure*: step only between grains, no ditches at the grain boundary
	ii. *Dual structure*: some ditches at the grain boundary in addition to steps, however, no single grain is completely surrounded by ditches
Unacceptable	*Ditch structure*: one or more grains is/are completely surrounded by ditches

Fig. 4 shows the microstructures of the HAZ of the weld track produced with a heat input less than 400J/mm etched in 10% oxalic acid. The microstructure show networks of grain boundary martensite (α') largely

unaffected by the oxalic acid etch except for partial ditching at the martensite-ferrite grain boundary (see the unattached arrow in the figure). Not a single grain boundary is found to be completely surrounded by ditches. Therefore, benchmarking the state of the microstructure in Fig. 4 with the criteria listed in Table 5 indicates that the weld track produced with heat input less than 400J/mm generally pass the sensitization test though the degree of partial ditching increases as the heat input increases.

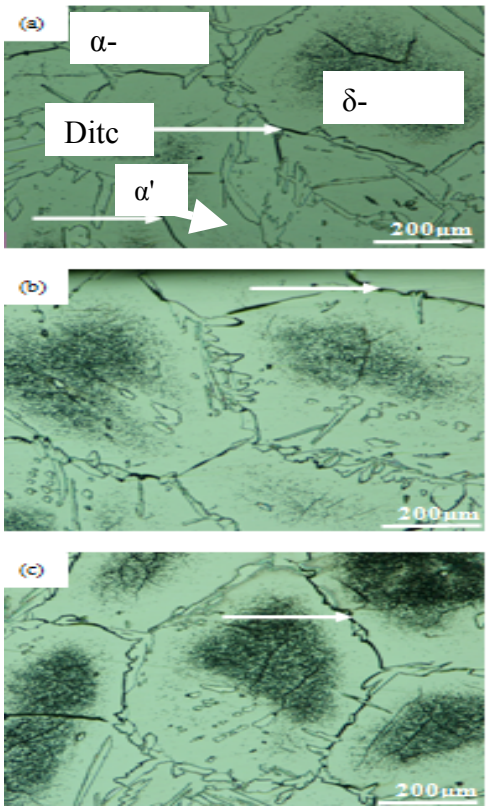

Fig. 4 Microstructure of the HAZ at heat input less than 400J/mm: (a) 288J/mm, (b) 336J/mm and (c) 370J/mm.

The oxalic acid etch response of the HAZ of the track produced with a heat input less than 500J/mm is shown in Fig. 5. The figure shows that the track produced with heat input of 403 J/mm show grain dropping on the martensite grain boundary while that produced with 436J/mm exhibit no ditched structure (Fig.5a and b). However, the track produced with 452J/mm clearly shows grains completely surrounded by ditches. Therefore, in relation to the acceptance criteria listed in Table 5, the weld track produced with heat input of 452J/mm is susceptible to sensitization. The ditched structure occurred on the ferrite-ferrite grain boundary while the ferrite-martensite phase boundaries are generally unaffected suggesting that the ferrite-martensite boundaries are not sensitized. This is in conformity with the observation of Greef and Du Toit [2] and Warmelo et al. [11] that carbide precipitation in ferritic stainless welds usually occurs on ferrite-ferrite grain boundary and rarely on ferrite-martensite boundaries.

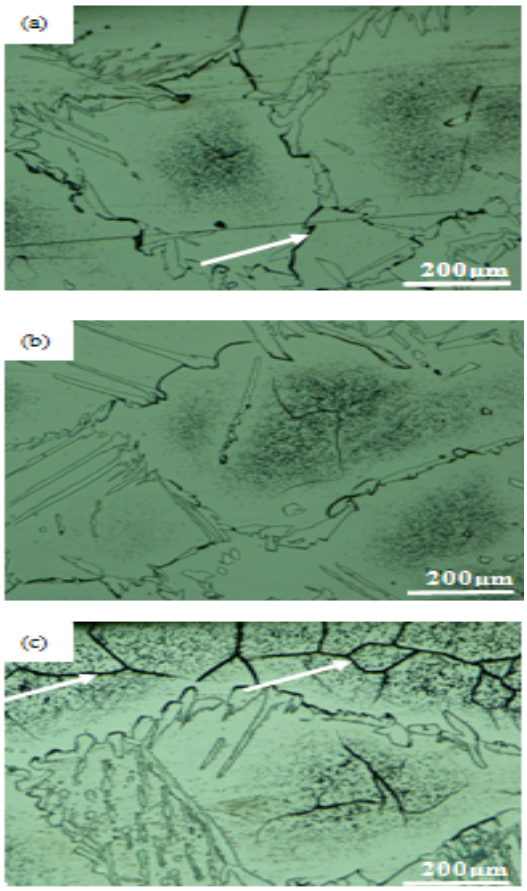

Fig. 5 Microstructure of the HAZ at heat input less than 500J/mm: (a) 403J/mm, (b) 432J/mm and (c) 452J/mm.

Fig. 6 gives the response of the weld tracks produced with heat input greater than 500J/mm to 10% oxalic acid etch. The figure show that the microstructure of the welds produced under this condition show extensive grain boundary ditching.

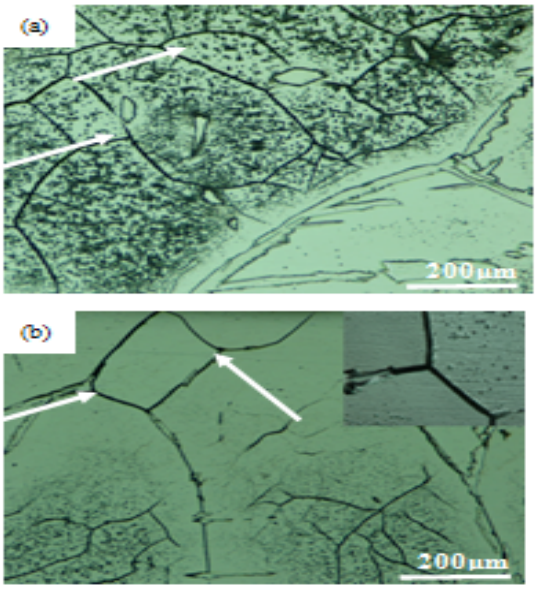

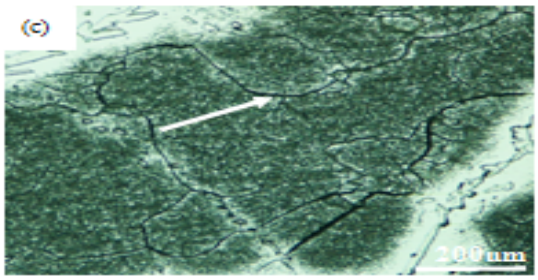

Fig. 6 Microstructure of the HAZ at heat input greater than 500J/mm: (a) 518J/mm, (b) 528J/mm and (c) 634J/mm.

The grain boundaries in these microstructures are continuously ditched with more than one grain completely surrounded by ditches (see Fig. 6b with insert of a close-up micrograph of the ditched grain boundary). The microstructure equally show that ditching also occur on the ferrite- martensite boundary particularly in those tracks produced with heat input of 528 and 634J/mm (see Fig. 6b and c). In relation to the classification criteria, these microstructures are in the sensitized condition and are therefore not acceptable.

Two broad streams of rating are apparent in this analysis. Weld tracks produced with heat input less than 452J/mm exhibit acceptable response to 10% oxalic acid etch while those produced with heat input greater than 450J/mm are susceptible to carbide precipitation. It thus appears that there is a relationship between heat input and susceptibility to carbide precipitation in 1.5mm thick medium chromium FSS welds. These microstructures validate the sensitization profile presented in Table 3 that sensitization increases in tracks made with higher heat input.

During welding, regions of the HAZ are exposed to differential peak temperatures of 650^0C and higher leading to different cooling rates. It was stated earlier that the peak temperature distribution in the thermal cycle and the time spent between these temperatures are critical parameters in evaluating the sensitization dynamics in the HAZ. These variables determine the degree of carbide precipitation [2, 7].

The peak temperature associated with the process parameters was calculated using Rosenthal's temperature profile of Eq. 3

$$T - T_0 = \theta_2 \left(\frac{\Delta t}{t}\right)^{1/2} \exp - \left(\frac{\theta_2^{\,2}\Delta t}{2e\left(T_p - T_0\right)^2}\right) \quad (3)$$

where T is the temperature at any given point in the HAZ, T_0 is the pre-weld temperature of the material before welding, Θ_2 is a dimensionless parameter, Δt is the cooling time from 1500-800^0C, t is instantaneous time in second, e is the base of the natural logarithm and T_p is the peak temperature of the thermal cycle; and the plot is provided in Fig.7. Similarly, the time spent (cooling rate) between these temperature regimes is shown in Fig.8.

Fig.7 shows that low heat input during welding induces drastic cooling and may shorten the time spend between the transformation temperatures. This inhibits δ → γ transformation producing a supersaturated delta-ferrite which eventually leads to carbide precipitation due to the absence of martensite to take carbon into solution. However, the KFF value of 14.7 for the material in relation to the Kaltenhausser specification indicates that martensite is present in the HAZ and therefore is expected to take carbon into solution and prevent sensitization.

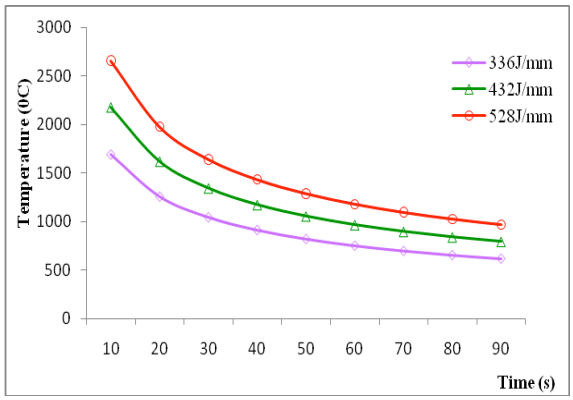

Fig. 7 Calculated thermal cycle in a point on the weld interface for different heat inputs.

Furthermore, Fig.8 shows that for comparative values of heat flux, the cooling rate increases with an increase in welding speed. Thus, weld tracks produced at intermediate and high heat fluxes with welding speeds of 2.5 and 3mm/s (452, 518, 528 and 634J/mm) experience slower cooling rates relative to tracks produced at low heat flux irrespective of the welding speed. This permits the diffusion of carbon from the matrix; and its subsequent combination with chromium to form chromium carbide which is precipitated on the ferrite-ferrite grain boundary.

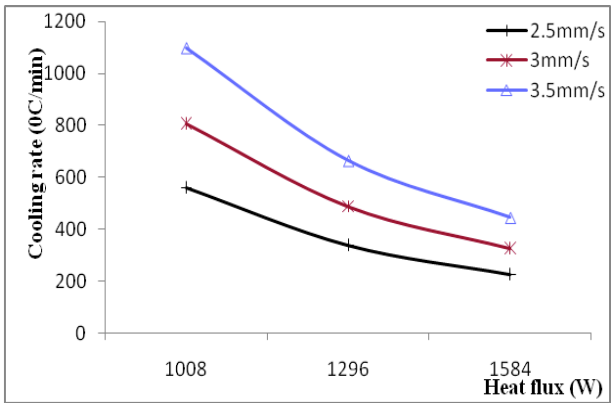

Fig. 8 Influence of heat fluxes and welding speed on cooling rate in the HAZ.

Greef and Du Toit [2] suggests that the maximum cooling time from 1500-800^0C to prevent sensitization in thin plate FSS weld should not exceed 8.75s. It is believed that cooling time longer than this promotes the

transformation of the high temperature austenite to low temperature ferrite which is supersaturated in carbon due to the low solubility of carbon in ferrite. This results in extensive carbide precipitation on the ferrite-ferrite grain boundaries during cooling.

The cooling times from 1500-800^{0}C associated with the welding conditions have been calculated and the values are provided in Table 3. The table show that the tracks produced with heat input of 452, 518, 528 and 634J/mm experienced cooling times greater than the suggested maximum of 8.75s and are therefore possibly in the sensitized condition. This condition is validated by the microstructures in Figs. 5c and 6. However, those made with a heat input less than 452J/mm spend less than the suggested 8.75s and are expected to be immuned to sensitization. This is supported by the microstructures presented in Figs.4 and 5(a, b).

4. Conclusions

The sensitization profile in medium chromium FSS welds produced under different welding conditions has been investigated. The following findings are apparent from the study:

i. The width of the sensitization zone increases with increasing the heat input. The depth of the sensitization zone in the thickness direction is insignificant and it is generally within one-half of a millimeter.
ii. The time spent within the sensitization region is critical to the size of the zone. The cooling time for the avoidance of carbide precipitation in the HAZ is around 9s. This is generally within the guideline provided in literature for thin plate FSS weld.
iii. The use of heat input greater than 432J/mm increases the development of sensitized regions. This level of heat input correspond to heat fluxes in the range 1008-1296W and welding speeds between 3mm/s and 3.5mm/s. Under this condition the average cooling time is about 10s.
iv. Most grain boundary attack is restricted to the ferrite-ferrite grain boundaries. The ferrite-martensite boundaries do not show visible attack. This indicates that welding conditions that promotes the formation of martensite in the HAZ are ideal for the prevention of sensitization.

Acknowledgement

Funding for the research documented in this paper came from the Research Management Office, International Islamic University Malaysia under Grant No EDW A11-020-0811.

References

[1] Lippold, J.C. and Kotecki, D.J. (2005), Welding Metallurgy and Weldability of Stainless steel, Wiley-Interscience, New Jersey, USA.
[2] Greef, M.L. and Du Toit, M. (2006), Looking at the sensitization of 11-12% chromium EN 1.4003 stainless steels during welding, Welding Journal, 85, p. 243s-251s.
[3] Amuda, M.O.H. (2008), unpublished PhD comprehensive examination document, Kulliyyah of Engineering, International Islamic University Malaysia, Gombak, 70p.
[4] Anbazhagan, V. and Nagalakshmi (2002), Metallurgical studies in ferritic stainless steel welds, Welding Research Journal, 23, p 25-37.
[5] Amuda M. O. H. and S. Mridha, (2010), Grain refinement in ferritic stainless steel welds: The journey so far, Advanced Materials Research, 83-86, p. 1165-1172.
[6] Amuda, M. O. H. and S. Mridha, (2011), Effect of energy input on microstructural features and mechanical properties of medium chromium ferritic stainless steel welds, in Proceedings International Conference on Materials Processing Technologies, June 2-3, Phuket, Thailand, p.77-84.
[7] Van Warmelo, M.N. (2007), Susceptibility of 12% Cr steels to sensitization during welding of thick gauge plate, unpublished M. Eng. Thesis, University of Wollongong, Australia, 106 p.
[8] Easterling, K. (1992), Introduction to Physical Metallurgy of Welding, 2nd ed., Butterworth Heinemann, Oxford.
[9] ASTM A763-93 (2004), Standard practices for detecting susceptibility to intergranular attack in ferritic stainless steel, ASTM International, p. 416-426.
[10] Tsai, N. S. and Eager. T. W. (1984), The size of the sensitization zone in 304 stainless steel welds, Journal of Materials for Heat Systems, 6(1), p. 33-37.
[11] Warmelo, M.W., Nolan, D. and Norish J. (2007), Mitigation of sensitization effects in unstabilized 12%Cr ferritic stainless steel welds, Materials Science and Engineering A, 464, p. 157-169.